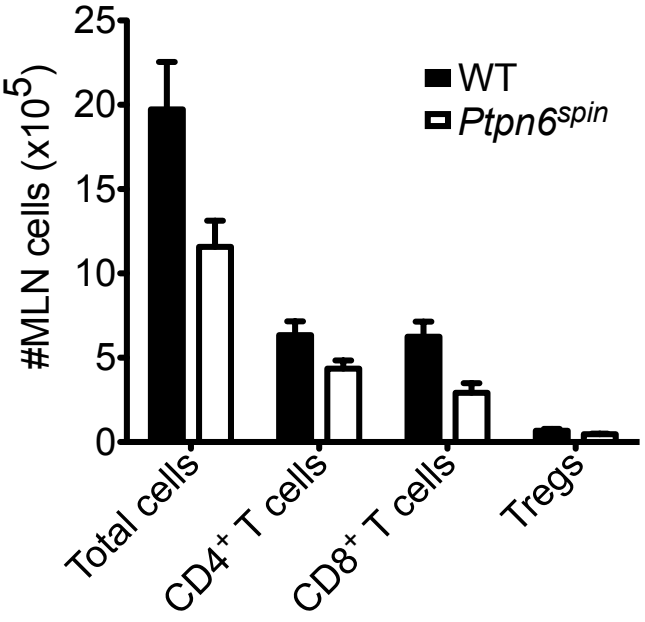

Supplementary Figure 1. Mutation in PTPN6 does not affect the accumulation of cells in non-skin draining LNs. Total numbers (mean ± s.e.m.) of cells in the mesenteric LNs (MLNs) of 14-16 week old WT (*n* = 4) and *Ptpn6*^{spin} (*n* = 4) mice that previously developed footpad disease. Data are representative of two independent experiments. Tregs refers to Foxp3 expressing CD4^{+} T cells.

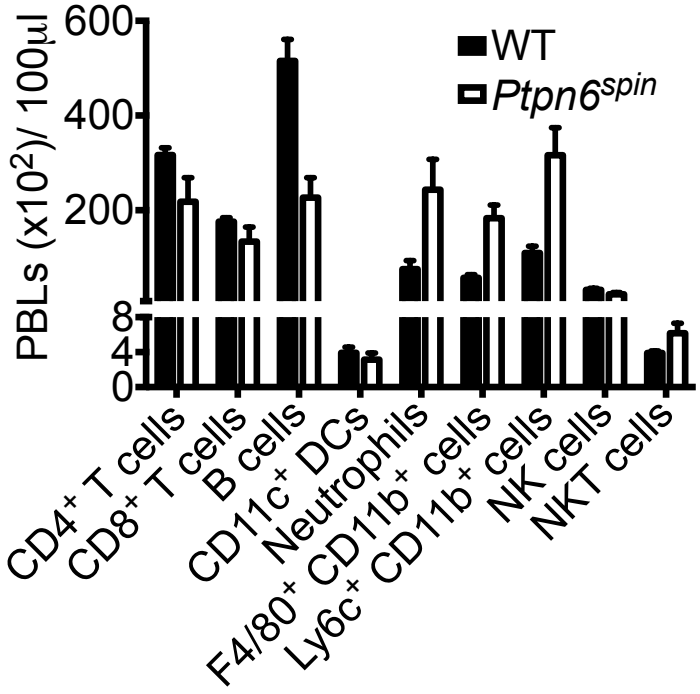

Supplementary Figure 2. *Ptpn6*^{spin} mutation results in enhanced numbers of circulating myeloid cells and neutrophils in the blood. Total numbers (mean ± s.e.m.) of circulating immune cells in equal volumes of peripheral blood from 12-16 week old WT (*n* = 5) and *Ptpn6*^{spin} (*n* = 5) mice that previously developed footpad disease. Data are representative of two independent experiments. PBL, peripheral blood leukocytes. DCs, dendritic cells. NK, natural killer.

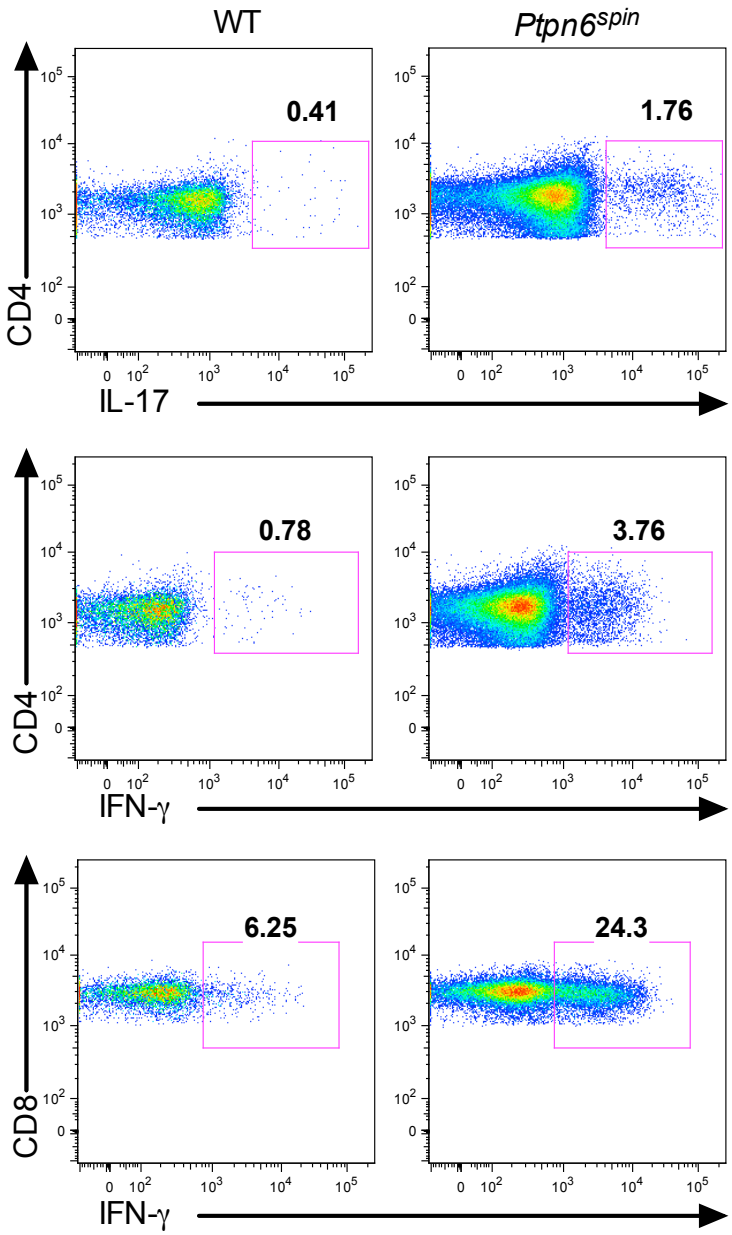

Supplementary Figure 3. The inflammatory environment in *Ptpn6*^{spin} mice promotes the generation of pathogenic T cells. PopLNs were harvested from 10-12 week old WT and diseased *Ptpn6*^{spin} mice and cells were restimulated with PMA/ionomycin followed by intracellular staining for IL-17 and IFN-γ. Representative FACs plots that correspond to the data presented in Figure 1f are shown. Data are representative of 5 independent experiments with at least 3-4 mice per group.

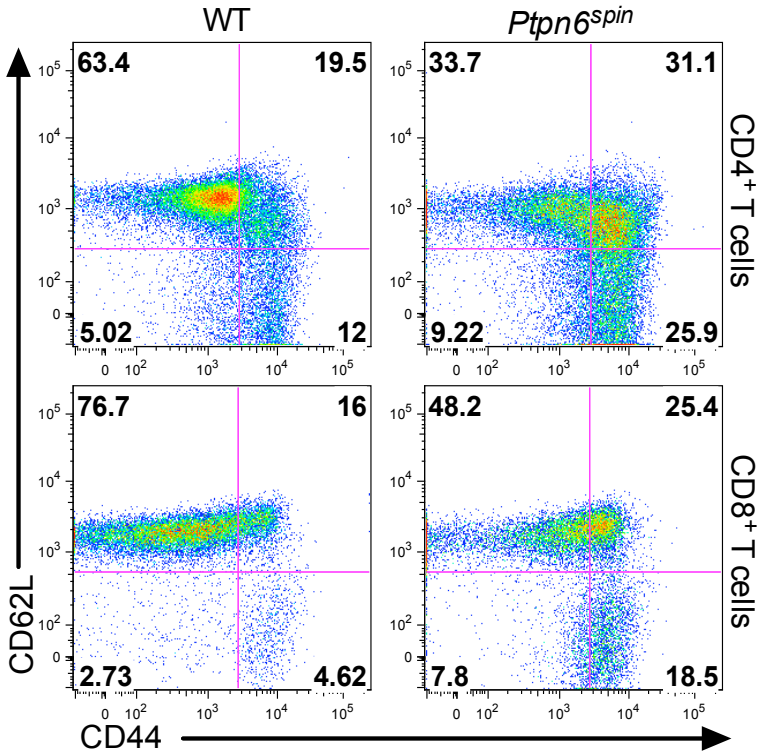

Supplementary Figure 4. T cells exhibit an effector/memory phenotype in diseased *Ptpn6*^{spin} mice. Expression of CD44 and CD62L by CD4$^+$ and CD8$^+$ T cells from the popLNs of WT and diseased *Ptpn6*^{spin} mice. Representative FACs plots from 5 independent experiments with at least 3-4 mice per group.

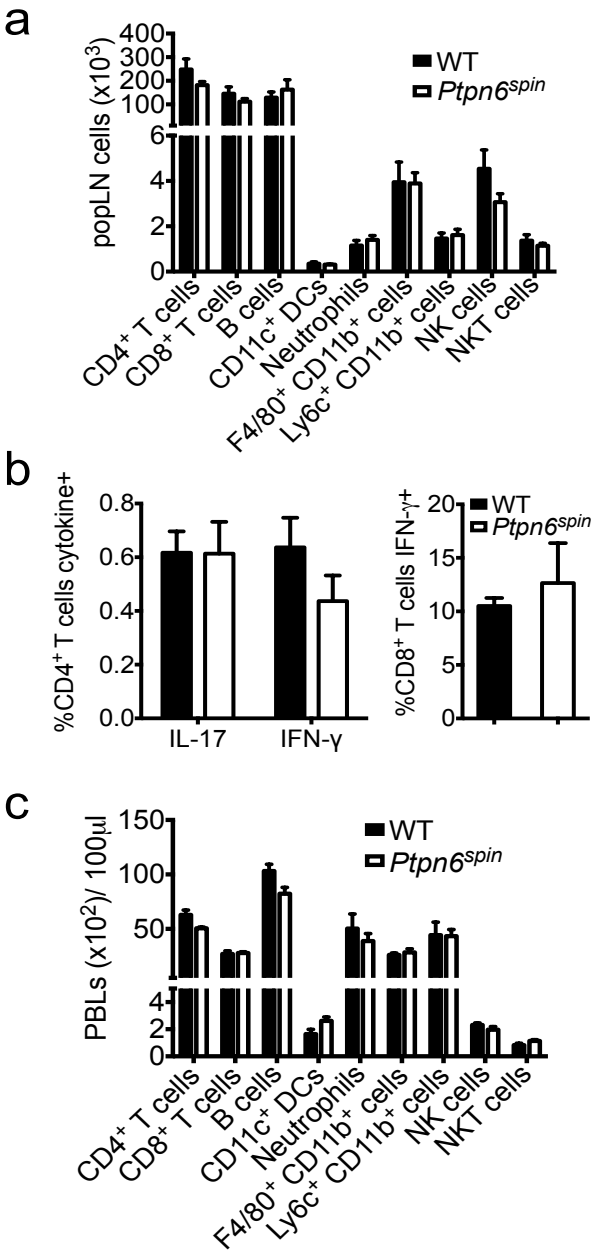

Supplementary Figure 5. Young *Ptpn6*^{spin} mice are characterized by normal numbers of immune cells. a-b, Cells were harvested from WT and disease-free *Ptpn6*^{spin} mice (4-8 weeks old). **a,** Numbers (mean ± s.e.m.) of popLN cells and **b,** production of cytokines by CD4$^+$ (left panel) and CD8$^+$ T cells (right panel) following brief restimulation. **c**, Total numbers (mean ± s.e.m.) of circulating immune cells in equal volumes of peripheral blood from 4-7 week old WT and *Ptpn6*^{spin} mice. PBL, peripheral blood leukocytes. DCs, dendritic cells. NK, natural killer.

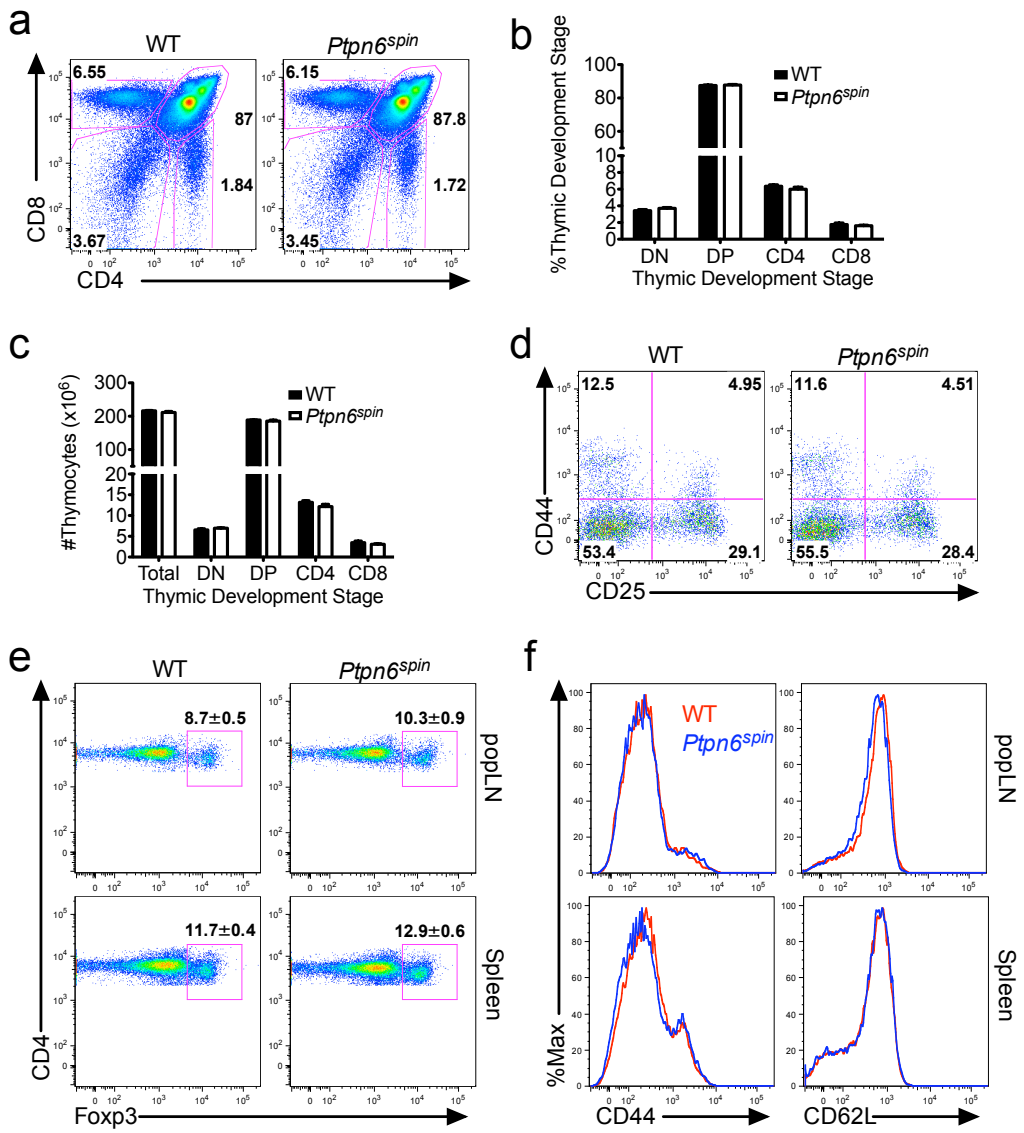

Supplementary Figure 6. PTPN6 mutation does not influence T cell development or peripheral T cell activation status before the onset of footpad disease. a-d, Thymic development was assessed in 4-7 week old WT and disease-free *Ptpn6*^{spin} mice. Representative FACs plots (**a**) and combined data (*n* = 3-4 mice per genotype) (**b**) of thymic development based on CD4 and CD8 staining. **c,** Total numbers (mean ± s.e.m.) of thymocytes in each stage of thymic development (*n* = 3-4 mice per genotype). DN, double negative (CD4$^-$ CD8$^-$); DP, double positive (CD4$^+$ CD8$^+$); CD4, CD4 single positive (CD4$^+$ CD8$^-$); CD8, CD8 single positive (CD4$^-$ CD8$^+$). **d,** Representative negative selection staining of double negative thymocytes. **e-f**, Analysis of the peripheral T cell compartment in 4-7 week old WT and disease-free *Ptpn6*^{spin} mice (*n* = 3-4 mice per genotype). **e,** Frequencies of CD4$^+$ T cells that express Foxp3 in the spleen and popliteal lymph nodes (popLN). **f,** Expression of CD44 and CD62L by CD4$^+$ T cells. All data are presented as mean ± s.e.m. Data are representative of 3 independent experiments.

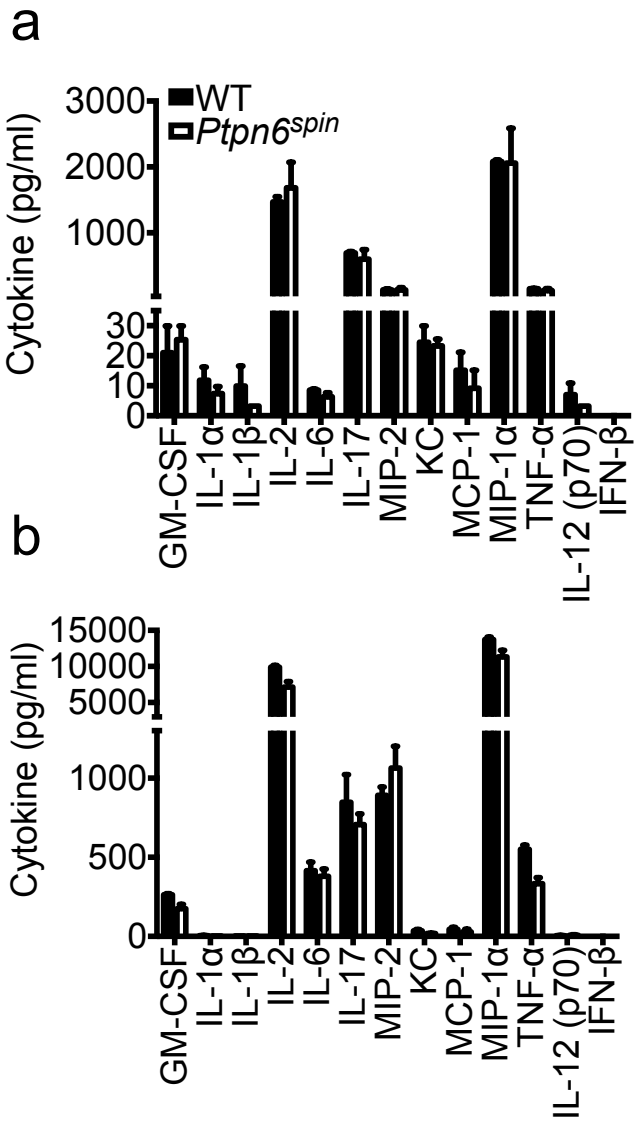

Supplementary Figure 7. PMA/ionomycin-induced cytokine secretion is not augmented in disease-free *Ptpn6*^{spin} mice. **a-b,** Popliteal lymph node cells (**a**) and splenocytes (**b**) from WT and young *Ptpn6*^{spin} mice (*n* = 3-4 mice per genotype) were stimulated with PMA/ionomycin for 24 hrs and the secretion of cytokines was measured by ELISA.

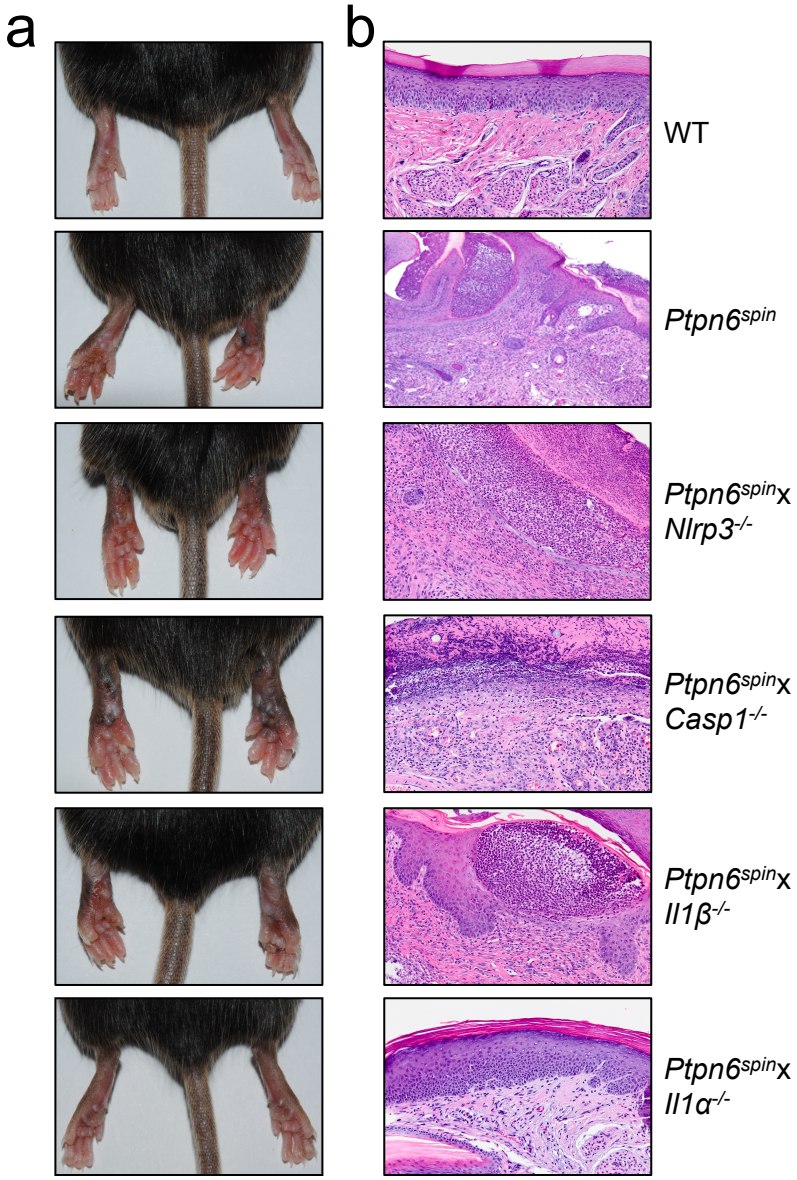

Supplementary Figure 8. Deletion of IL-1α abrogates cutaneous inflammatory disease in *Ptpn6*^{spin} mice. a-b, Footpad images (**a**) and H&E sections (**b**) of WT and *Ptpn6*^{spin} mice that were crossed with mice that are deficient in either NLRP3, Caspase-1, IL-1β, or IL-1α. Representative images and sections are shown.

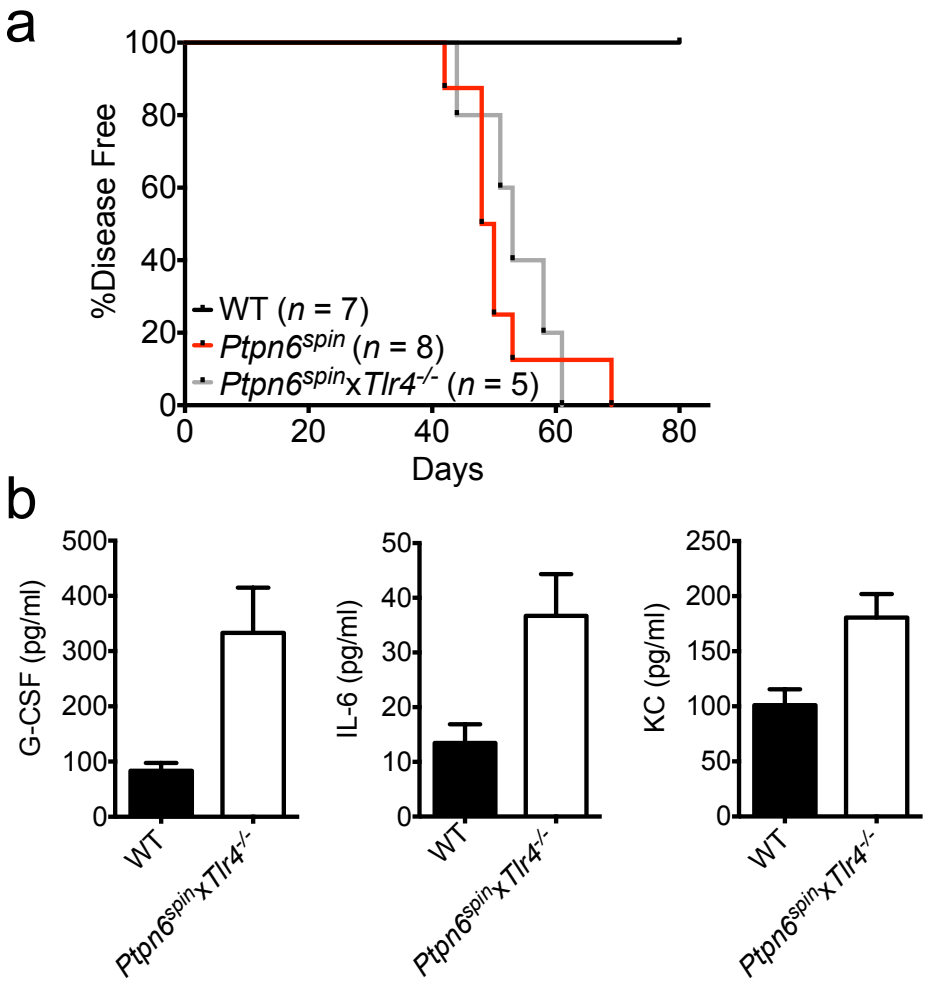

Supplementary Figure 9. Deletion of TLR4 does not provide protection against *Ptpn6^{spin}*-mediated disease. a, Incidence of spontaneous inflammatory footpad disease in WT, *Ptpn6^{spin}*, and *Ptpn6^{spin}*x*Tlr4$^{-/-}$* mice over time. **b,** Serum cytokine levels in WT and *Ptpn6^{spin}*x*Tlr4$^{-/-}$* mice at 10-14 weeks of age.

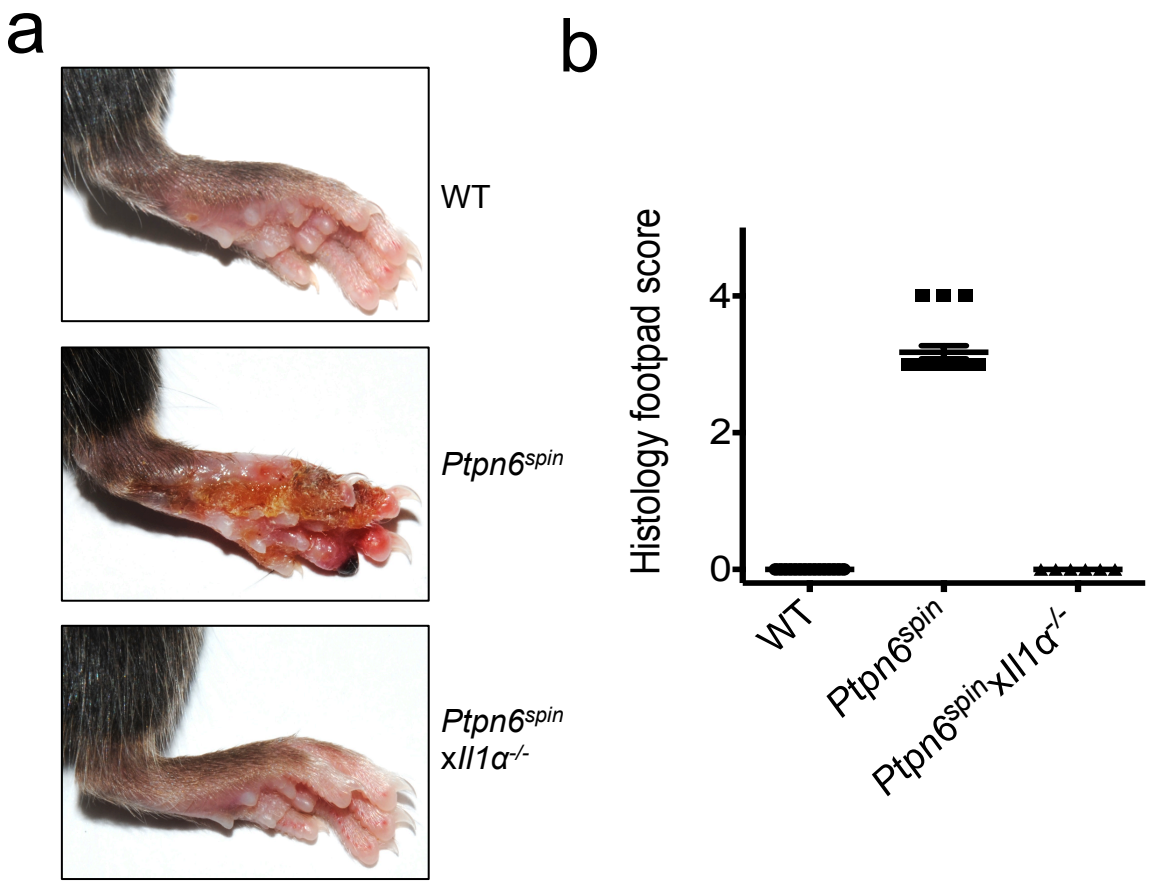

Supplementary Figure 10. IL-1α deficiency protects *Ptpn6^{spin}* mice from footpad pathology. a, Representative footpad images of microabrasion mice at 3-4 weeks post wound induction. **b**, Footpad H&E sections at 3-4 weeks post microabrasion wound induction were scored based on the extent and severity of inflammation, ulceration, and hyperplasia of the mucosa in a blinded fashion by a veterinary pathologist. Each point represents an individual mouse, and the line represents the mean ± s.e.m. Data are combined from two independent experiments.

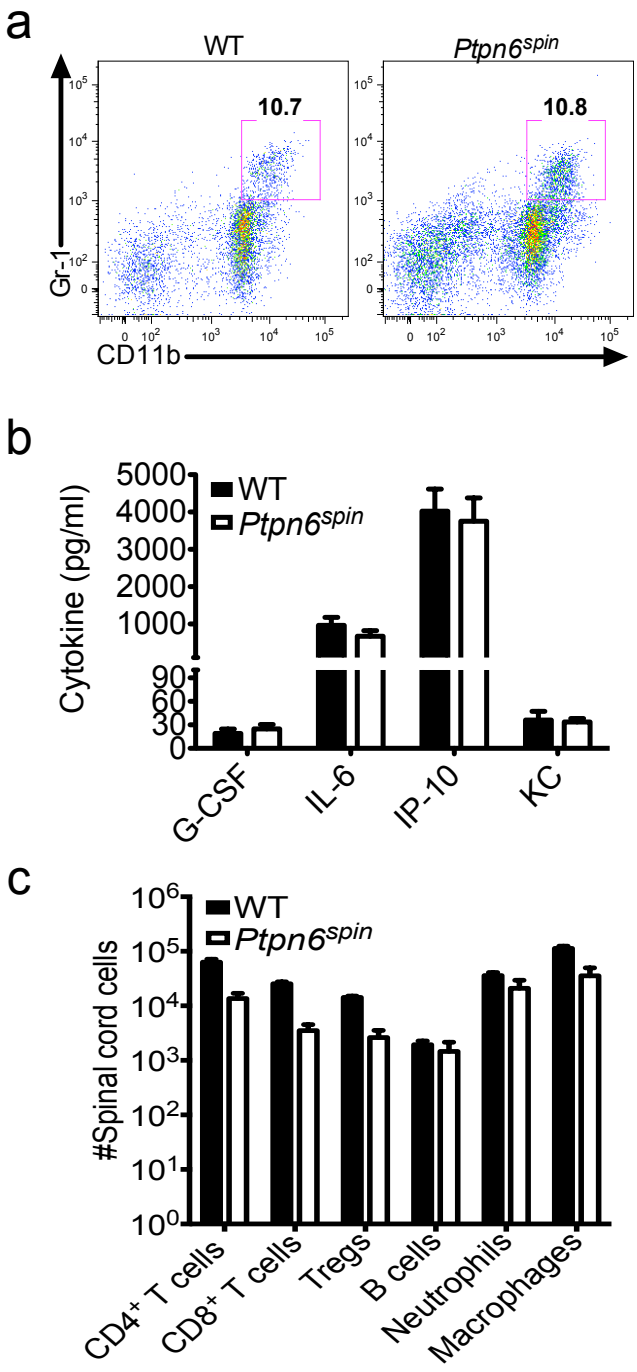

Supplementary Figure 11. PTPN6 mutation does not influence neuroinflammation during EAE. **a-c,** WT and disease-free (4-7 weeks of age) *Ptpn6*^{spin} mice were immunized with MOG/CFA and leukocytes from the spinal cord were harvested on day 20. **a,** Frequencies of neutrophils (CD11b^{+} Gr-1^{+} cells) in the CD45^{+} population. **b,** Spinal cord cells were stimulated for 48 hrs with MOG peptide and granulopoietic cytokines were measured by ELISA. **c**, Numbers (mean ± s.e.m.) of cells in the spinal cord at day 20. Data are representative of two independent experiments with at least 3-4 mice per group. Data show mean ± s.e.m.

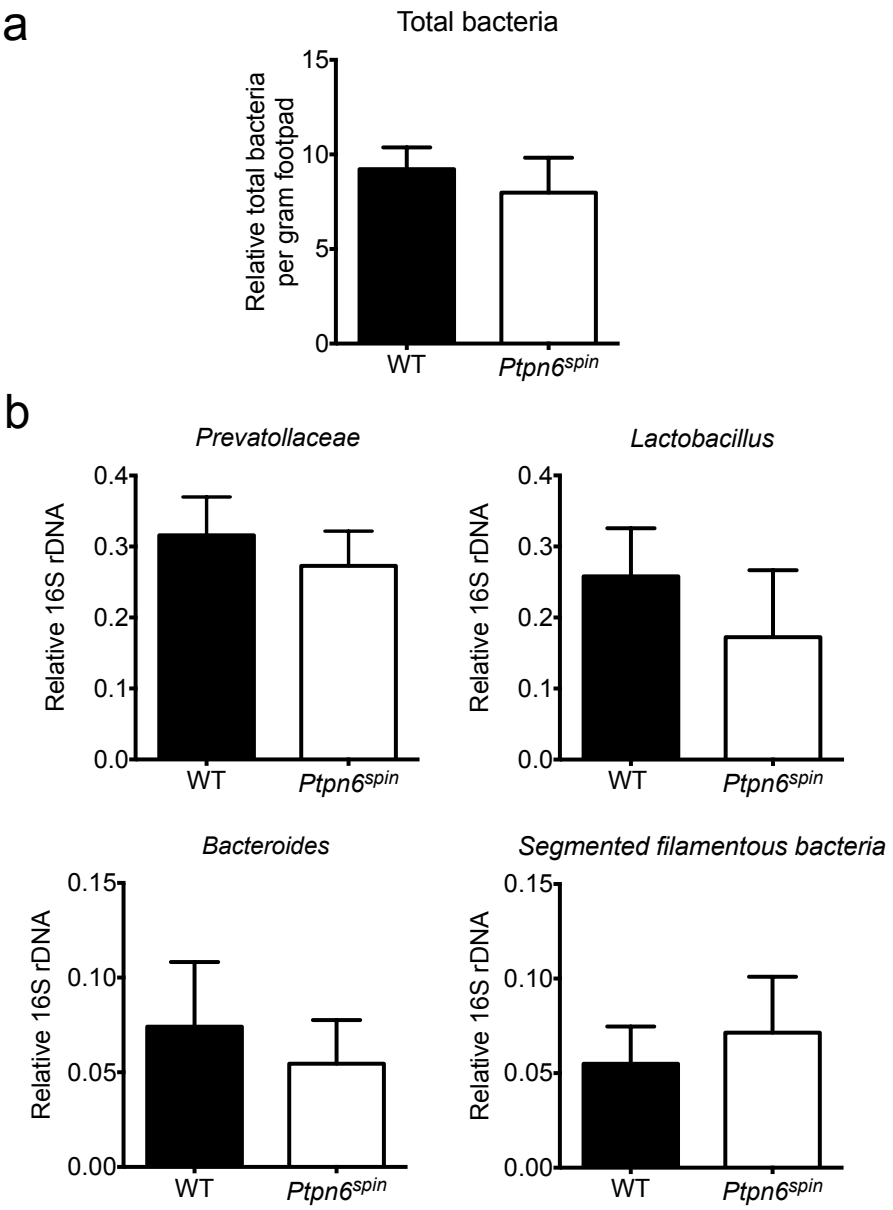

Supplementary Figure 12. Commensal skin bacteria composition is not altered in *Ptpn6*^{spin} mice. a-b, Levels of total bacteria (**a**) and specific bacterial species (**b**) in the skin of WT and diseased *Ptpn6*^{spin} mice (12-16 weeks of age). The bar graphs show mean ± s.e.m.

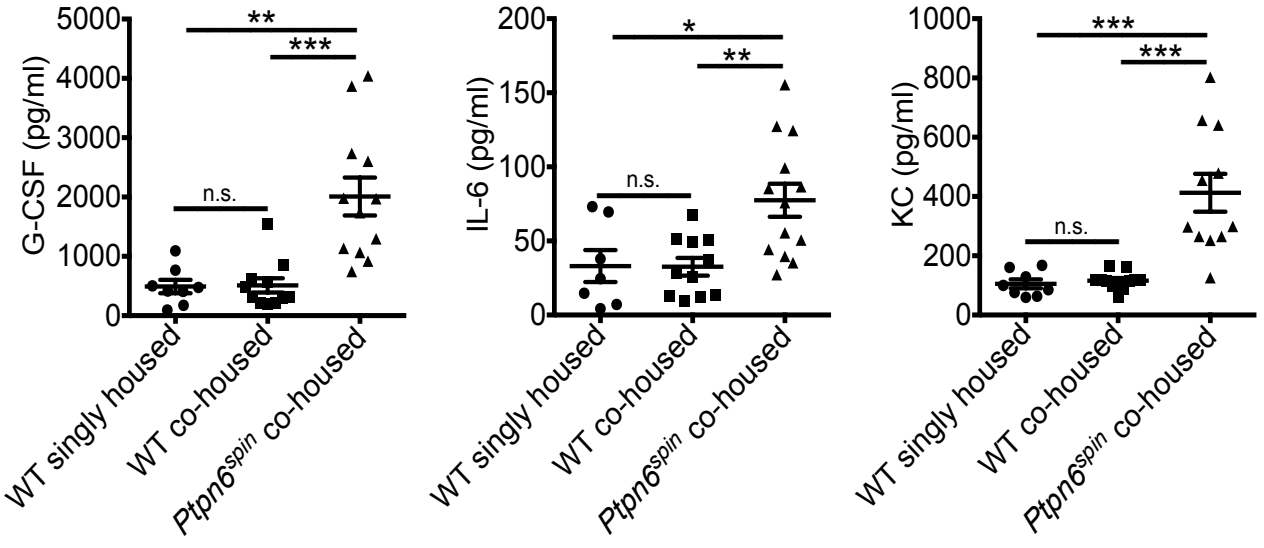

Supplementary Figure 13. *Ptpn6*^{spin}-mediated inflammatory disease is not transferrable to WT mice. WT mice were singly housed or co-housed at a 1:1 ratio with *Ptpn6*^{spin} mice immediately following birth. The levels of serum cytokines and chemokines were determined in mice at 10-16 weeks of age. Each point represents an individual mouse, and the line represents the mean ± s.e.m. **P* < 0.05, ***P* < 0.01, ****P* < 0.001. n.s., not statistically significant. Data are representative of two independent experiments.

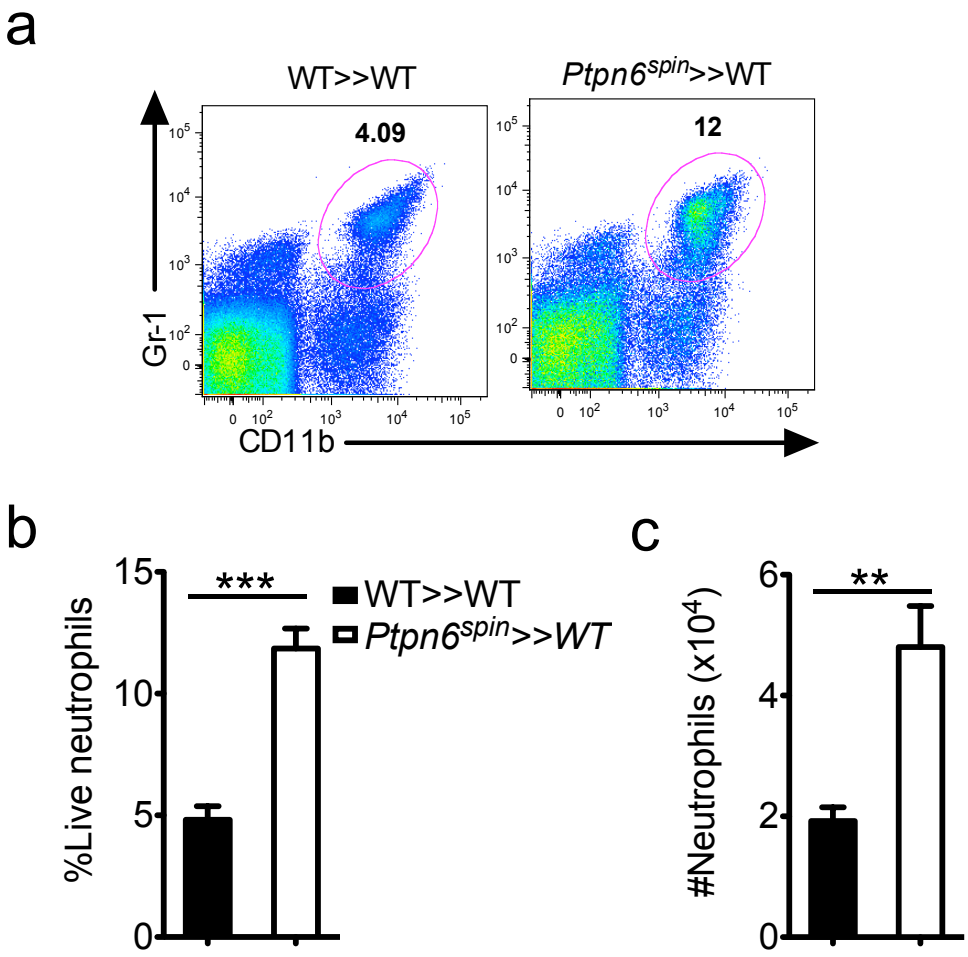

Supplementary Figure 14. *Ptpn6*^{spin} mutation in the haematopoietic compartment causes neutrophilia. **a-c,** Bone marrow chimera mice (donor>>recipient) were generated and the levels of circulating neutrophils in the blood was determined. Representative FACs plots (**a**) and combined data (*n* = 3-4 mice per chimeric group) (**b**) depicting the frequencies of circulating cells in the blood that are CD11b^{+} Gr-1^{+} neutrophils. **c,** Enumeration of circulating neutrophils in equal volumes of blood.

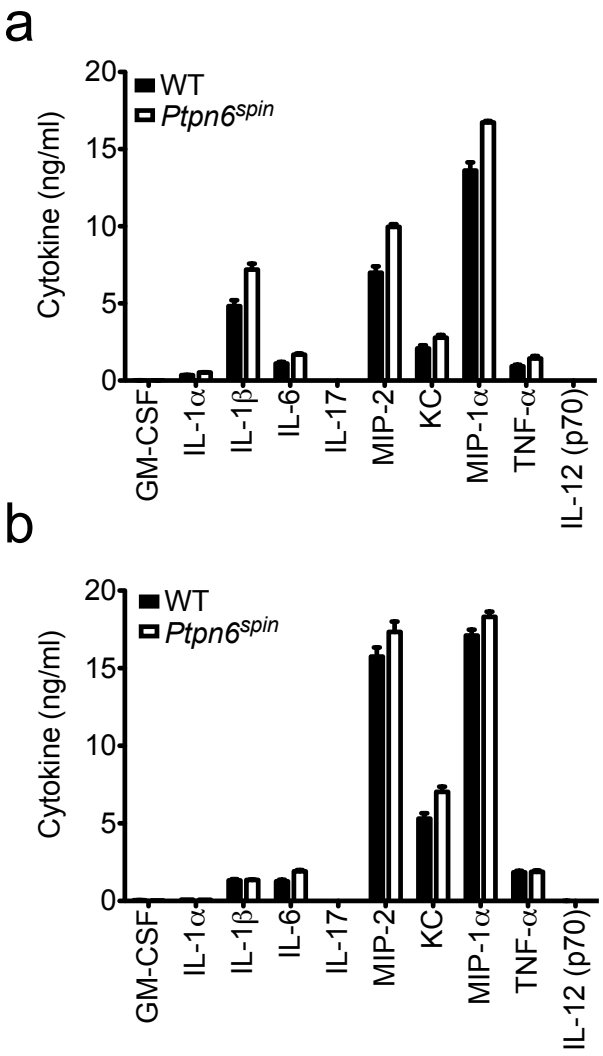

Supplementary Figure 15. Macrophage-mediated production of proinflammatory cytokines is not affected by PTPN6 mutation. a-b, Bone marrow derived macrophages (BMDMs) were stimulated with either LPS followed by ATP (**a**) or *Salmonella typhimurium* (5 MOI) (**b**) for 4 hr and supernatants were collected to evaluate cytokine secretion by ELISA. The bar graphs show mean ± s.e.m. of triplicate wells. Data are representative of four independent experiments.

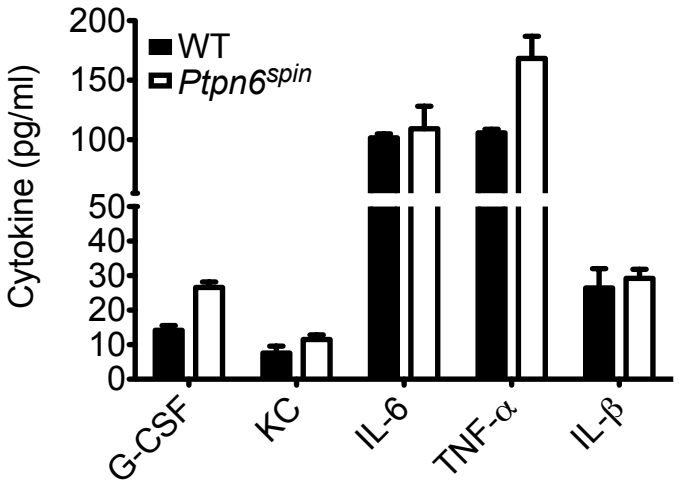

Supplementary Figure 16. PTPN6 mutation in neutrophils results in slightly higher levels of proinflammatory cytokine secretion. Purified WT and *Ptpn6*^{spin} neutrophils were isolated via flow cytometry sorting. Neutrophils were stimulated with LPS for 48 hrs and cytokine secretion was measured by ELISA. The bar graphs show mean ± s.e.m. of triplicate wells. Data are representative of three independent experiments.

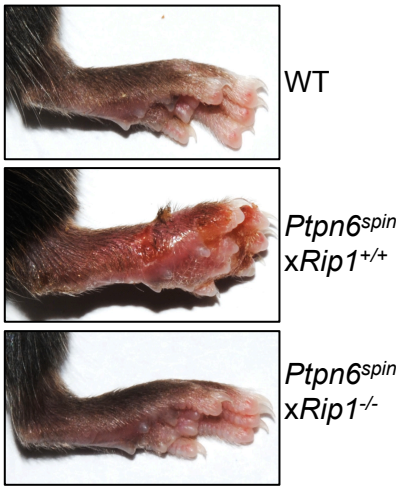

Supplementary Figure 17. Genetic ablation of RIP1 limits *Ptpn6^{spin}*-mediated skin disease. Representative footpad images of WT (*Ptpn6^{WT}*x*Rip1$^{+/+}$* >> WT), *Ptpn6^{spin}*x*Rip1$^{+/+}$* (*Ptpn6^{spin}*x*Rip1$^{+/+}$* >> WT), and *Ptpn6^{spin}*x*Rip1$^{-/-}$* (*Ptpn6^{spin}*x*Rip1$^{-/-}$* >> WT) fetal liver transplant mice (donor>>recipient).

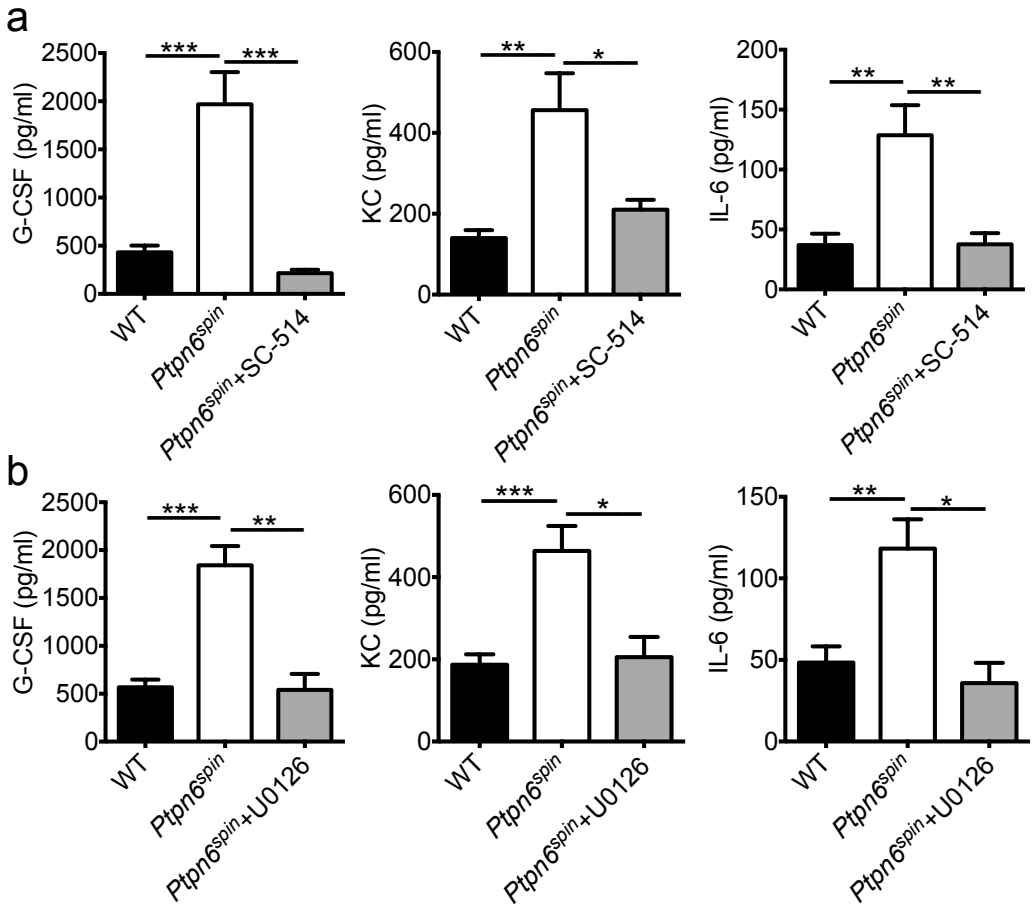

Supplementary Figure 18. Inhibition of NF-κB and ERK signalling rescues aberrant cytokine production in *Ptpn6^{spin}* mice. WT mice were pretreated with vehicle control (n = 11-26) and *Ptpn6^{spin}* mice were pretreated with vehicle control (n = 14-26), 150 μg of SC-514 (n = 10) (**a**) or 75 μg of U0126 (n = 7) (**b**) for 1 hour before microabrasion injury induction. Serum levels of granulopoiesis-inducing factors 5 hrs post wound induction. The bar graphs show mean ± s.e.m. *P < 0.05, **P < 0.01, ***P < 0.001.

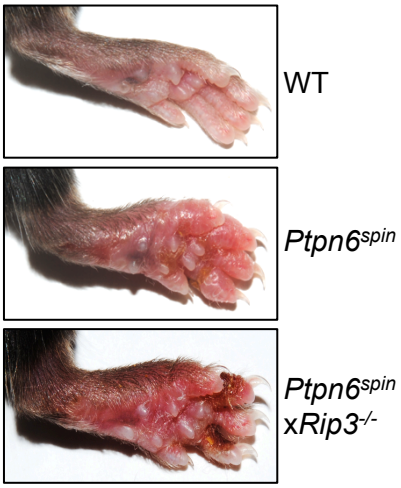

Supplementary Figure 19. RIP1-mediated regulation of inflammation in *Ptpn6^{spin}* mice is not through its regulation of RIP3-induced necroptosis. Microabrasion injuries were induced on the plantar surfaces of the footpads of WT, *Ptpn6^{spin}*, and *Ptpn6^{spin}*x*Rip3$^{-/-}$* mice. Representative footpad images of mice at 4 weeks post wound induction are depicted.